

Screw dislocation cross slip at cross-slip plane jogs and screw dipole annihilation in FCC Cu and Ni investigated via atomistic simulations



S.I. Rao^{b,e,*}, D.M. Dimiduk^c, J.A. El-Awady^d, T.A. Parthasarathy^b, M.D. Uchic^a, C. Woodward^a

^a Air Force Research Laboratory, Materials and Manufacturing Directorate, AFRL/RXCM, Wright-Patterson AFB, OH 45433-7817, United States

^b UES, Inc., 4401 Dayton-Xenia Rd, Dayton, OH 45432-1894, United States

^c BlueQuartz Software, LLC, 400 S. Pioneer Blvd, Springboro, OH 45066, United States

^d Department of Mechanical Engineering, Johns Hopkins University, Baltimore, MD, United States

^e Institute of Mechanical Engineering, EPFL, Lausanne 1015, Switzerland

ARTICLE INFO

Article history:

Received 12 August 2015

Revised 13 August 2015

Accepted 29 August 2015

Keywords:

Cross-slip

Jogs

Screw dipole annihilation

Atomistic simulations

Nickel

Copper

ABSTRACT

Using atomistic simulations, the effect of jogs on the cross-slip of screw character dislocations and screw-dipole annihilation was examined for both FCC Cu and Ni. The stress-free activation energy for cross-slip at jogs is close to 0.4 eV in Cu, determined using a nudged elastic band method. This value is a factor of 4-to-5 lower than the activation energy for cross-slip of screw dislocations in the absence of a jog. Similar results were obtained for Ni. Molecular dynamics simulations were used to study the annihilation of a jog-containing screw dipole. The critical Escaig stress on the glide plane for dipole annihilation drops quickly from the 0 K value of ~ 400 MPa and, dipole annihilation is nearly athermal at room temperature. At 5 K, Escaig stresses on the cross-slip plane are a factor of 1.5 less effective than Escaig stresses on the glide plane and, glide stresses on the cross-slip plane are a factor of 3 less effective for dipole annihilation by cross-slip. The activation volume for cross-slip of screw dislocations at jogs with respect to these three stress components range from 6 to $20b^3$. These results have been found to be useful in physics-based modeling of bulk cross-slip in higher length scale 3D dislocation dynamics simulations investigating dislocation pattern formation and fatigue structures in FCC crystals.

© 2015 Acta Materialia Inc. Published by Elsevier Ltd. All rights reserved.

1. Introduction

Cross-slip of screw character dislocations is an elementary thermally-activated mechanism that is all prevalent in plastic deformation. The consequences of cross slip are recognized as the most important single process underlying complex spatiotemporal development of dislocation microstructure leading to hardening, pattern formation and dynamic recovery [1,2]. The early work of Escaig remains the most widely cited and used model for cross-slip [3–7]; however, this model poses several difficulties with respect to quantitative simulations [8–12]. Previously, atomistic simulations (molecular statics) were used with embedded atom potentials to evaluate the activation barrier for a screw dislocation to transform from fully residing on the glide plane to fully residing on the cross-slip plane, where the screw dislocation was intersecting a mildly-attractive 120° forest dislocation forming Glide locks (GL), Lomer–Cottrell (LC) locks, or Hirth locks, in both Ni and Cu [8,9]. The cross-slip process was also explored at

mildly-repulsive screw dislocation intersections [12]. In these simulations, the Burgers vector of the intersecting dislocation forming mildly attractive GL or LC locks was reversed. The activation energies at attractive intersections were computed using two different techniques: (a) determine the equilibrium configurations (energies) when varying pure tensile or compressive stresses that are applied along the [111] direction on the partially cross-slipped state, and (b) the classical nudged elastic band method. The cross-slip activation energies at the attractive intersections were found to be a factor of 3–20 lower than the energy for cross-slip at an isolated screw dislocation. At mildly repulsive intersections, cross-slip nucleation was found to be spontaneous and athermal, with zero cross-slip activation energy [12]. These findings provide a better physical basis to represent local cross-slip processes in larger-scale, discrete dislocation-dynamics simulations, enabling more realistic simulations of the evolution of the dislocation substructure. Such simulations should result in improved statistical representation of cross-slip effects during monotonic or cyclic deformation.

In addition, previously Vegge et al. considered cross-slip nucleation and screw dipole annihilation at two types of atomic jogs in FCC Cu [13,14]. They evaluated the activation energy for cross-slip

* Corresponding author at: Institute of Mechanical Engineering, EPFL, Lausanne 1015, Switzerland.

E-mail addresses: car894@aol.com, raosatish806@gmail.com (S.I. Rao).

at atomic jogs using a nudged elastic band method, and found that the activation energy for cross-slip decreases by a factor of 3 as compared to cross-slip of screw dislocations in isolation. The results were identical for both types of jogs. They also evaluated the critical dipole annihilation distance of jogged-screw dislocations and found it to be 4 nm at 0 K. However, these calculations were performed using an interatomic potential that does not give the correct elastic constants and stacking fault energy of Cu (shear modulus 20% higher and stacking fault energy 30% lower than experimental values). Also, the temperature and stress dependence of cross-slip nucleation and dipole annihilation at jogged-screw dislocations was not considered.

In this study, cross-slip nucleation is examined at atomic jogs on screw dislocations using Mishin's interatomic potentials for Ni and Cu, which give elastic constants and stacking fault energies close to experimental values. The line direction of the jog resides on the cross-slip plane. It is argued that all types of atomic jogs on screw dislocation can be decomposed into a jog on a cross-slip plane plus a kink on the glide plane. Therefore, we have only considered one type of atomic jog on a cross-slip plane for calculating the cross-slip activation energy, as well as for the screw-dipole annihilation simulations. The annihilation of jogged-screw dipoles having initial separations of 14 and 44 nm were also simulated. The critical Escaig stresses for cross-slip nucleation and screw-dipole annihilation, as a function of temperature, were determined using molecular dynamics simulations. The remainder of this paper is organized as follows. Section 2 describes the simulation technique, the interatomic potentials used in the simulations, and briefly describes the method used to both analyze and visualize the core structures. Section 3 contains the results of the simulations, Section 4 presents a brief discussion of the results, and Section 5 gives a summary of the results.

2. Simulation technique

The atomistic simulations described here employed the 3-dimensional (3D) parallel molecular dynamics code, LAMMPS [15], developed at Sandia National Laboratory. The dimensions of the simulation cell were $200.0 \times 20.0 \times 100.0$ nm along the x -, y -, and z -axes, respectively. The x -axis was aligned parallel to the $[785, -783, 2]$ crystallographic direction, which corresponded to the line direction of a screw dislocation $[1-10]$ offset by a $\frac{1}{2}[011]$ vector resolved on the $(11-1)$ cross-slip plane. The z -axis was aligned parallel to the $(11-1)$ cross-slip plane normal, and the y -axis was aligned along the $[-781, -787, -1568]$ direction. In total, the simulation cell had approximately 34 million atoms. Periodic boundary conditions were applied along the x direction.

A single screw dislocation having a Burgers vector $\frac{1}{2}[1-10]$ was inserted into the simulation cell to examine the effect of jogs on the energetics of cross-slip. The elastic center of the initial anisotropic displacement field was selected such that the screw dislocation, upon molecular statics relaxation using fixed boundary conditions along the y and z directions, dissociates into Shockley partials on the (111) glide plane. Since the periodic direction is offset by a jog vector on the $(11-1)$ cross-slip plane, with respect to the screw direction, a jog on the cross-slip plane naturally forms upon such relaxation.

Selected loading configurations were used to calculate the energetics associated with cross-slip at the atomic jog. Uniaxial stress along the cross-slip plane normal, $[11-1]$ direction, was applied to generate Escaig stress on the (111) glide plane. The Escaig stresses act to expand or constrict the Shockley partials, depending on the sense of the stress, independent of the glide or cross-slip plane stresses. Note that uniaxial stress along this particular crystallographic direction results in no Escaig stress component on the

$(11-1)$ cross-slip plane as well as no glide stresses on both the glide and cross-slip planes. Similarly, uniaxial stress along the glide plane normal, $[111]$ was applied to generate Escaig stress on the $(11-1)$ cross-slip plane without any Escaig stress on the (111) glide plane, as well as no glide stress on both the glide and cross-slip planes. Equal uniaxial stresses along the $[10-1]$ and $[0-11]$ directions were used to generate pure glide stresses on the $(11-1)$ cross-slip plane without any glide stresses on the (111) glide plane, as well as no Escaig stress on either glide or cross-slip planes. Such uniaxial stresses were applied using appropriate uniform straining of the dislocated lattice, and using fixed boundary conditions along the y and z directions.

To examine the effect of atomic jogs on the energetics of cross-slip annihilation of screw dipoles, a pair of oppositely-signed screw dislocations was inserted into the simulation cell separated along the y direction by 14 or 44 nm. In some simulations, the screw dislocations were also offset along the $[11-2]$ direction on the (111) glide plane, such that they tended to move toward each other on their respective glide planes under the action of both interaction and applied forces. For these simulations, the dimension of the simulation cell along the z direction was increased to ~ 100.0 nm, corresponding to a total of ~ 170 million atoms in the simulation cell. In addition, a different simulation cell was used to examine screw dipoles where a jog was present on only one of the dislocations. In this case, the x -axis was aligned along the $[1-10]$ direction and the y -axis along $[-1-1-2]$. On one half of the simulation cell, as described previously, a pair of oppositely-signed screw dislocations was inserted separated along the z direction by 14 or 44 nm. On the other half of the simulation cell, one of the screw dislocations was displaced with respect to the other half by a jog vector on the cross-slip plane while the other screw dislocation was continuous with the other half. Each half-cell was relaxed separately using periodic boundary conditions along the x direction. Finally, the two halves were brought together and relaxed using fixed boundary conditions along the x direction. This procedure generated a jog vector on only one of the screw dislocations.

In the molecular dynamics (MD) simulations, free-surface boundary conditions were applied along the y and z directions. Additional forces were applied on atoms in a thin layer (twice the range of the interatomic interactions in the EAM potential) at both boundaries along the y and z directions. The sum of the individual atom forces at each boundary along the y and z directions was equal and opposite and, corresponded to the applied stress state in the initial molecular statics simulation cell. The initial conditions for the MD simulations were a molecular statics relaxed cell under stress.

2.1. Interatomic potentials

The embedded atom interatomic potentials used for the simulations are those developed for FCC Ni and Cu by Mishin et al. [16,17]. Table 1 shows the lattice parameter, cohesive energy, elastic constants and stacking fault energy produced by the Ni and Cu potentials. The Shockley partial spacing width, d , for the screw dislocation is $d/b = 4-5$ for the Ni potential and $d/b = 6$ for the Cu potential, where b is the magnitude of the Burgers vector, \mathbf{b} , of the screw dislocation. The lattice parameter, cohesive energy, elastic constants and stacking-fault-energy values are very near experimental values, and therefore the results from using these potentials should be representative for these metals.

2.2. Depiction of core structures

For depiction and visualization of the dislocation core structures, we used the method developed by Stukowski and Albe [18] to analyze the atomistic simulations. The method extracts dis-

Table 1

Lattice constant, a_0 , cohesive energy, E_c , elastic constants, C_{11} , C_{12} and C_{44} , stacking fault energy, γ , and Shockley partial splitting of the screw dislocation, d/b , given by the Mishin Ni and Cu potentials.

	Mishin (Ni)	Mishin (Cu)
a_0 (Å)	3.52	3.615
E_c (eV)	−4.45	−3.54
C_{11} ($\times 10^{11}$ N/m ²)	2.413	1.699
C_{12} ($\times 10^{11}$ N/m ²)	1.508	1.226
C_{44} ($\times 10^{11}$ N/m ²)	1.273	0.762
γ (mJ/m ²)	134	44
d/b	4–5	6

location lines and their associated Burgers vectors from three-dimensional atomistic simulations. This method is based on a fully automated Burgers circuit analysis that first locates the dislocation cores and subsequently determines their Burgers vector. The transition from the atomistic system to a discrete dislocation representation is achieved through a vectorization step. Sophisticated information, including dislocation reactions and junctions, can be obtained from this type of analysis.

3. Decomposition of atomic-scale dislocation line off-sets

If the screw dislocation is assumed to have a Burgers vector of $\frac{1}{2}[1-10]$ and its glide plane is taken to be (111) , i.e. the screw dislocation is dissociated into Shockley partials on this glide plane, then the cross-slip plane becomes $(11-1)$. For any jog (that by definition has a line vector that is out of the screw-direction glide plane), it can be shown that this jog can dissociate into a jog vector on the cross-slip plane and a kink vector on the glide plane. For example, if one considers the $[001]$ vector, a possible decomposition is the creation of a $\frac{1}{2}[101]$ jog vector on the cross-slip plane and a $\frac{1}{2}[-101]$ kink vector on the glide plane. An alternate decomposition is creation of a $\frac{1}{2}[011]$ jog vector on the cross slip plane and a $\frac{1}{2}[0-11]$ kink vector on the glide plane. Similarly, a $[010]$ vector can be decomposed into a $\frac{1}{2}[011]$ vector on the cross-slip plane and a $\frac{1}{2}[01-1]$ vector on the glide plane. It can also be $\frac{1}{2}[011]$ vector on the cross-slip plane and a $\frac{1}{2}[10-1]$ vector on the glide plane, or it can decompose into a $\frac{1}{2}[-110]$ vector – which is common to both glide and cross-slip planes – and a $\frac{1}{2}[110]$ vector. The $\frac{1}{2}[110]$ vector, in turn, can dissociate into a $\frac{1}{2}[101]$ vector on the cross-slip plane and a $\frac{1}{2}[01-1]$ vector on the glide plane. Between the types of decompositions listed above, a dislocation would always decompose into the configuration having a minimum energy (between obtuse and acute jog vectors). This suggests that for any atomic offset vector on the screw dislocation, the offset vector would always contain a jog vector on the cross-slip plane, plus usually a kink vector on the glide plane. Therefore, the cross-slip activation energy and activation stress as a function of temperature needs to be computed only at a single atomic jog vector on the screw dislocation. This jog-kink decomposition is suggested to be the reason as to why in previous studies, Vegge et al. [12,13] found almost identical cross-slip activation energies and jog-segment mobilities at both $\frac{1}{4}\langle 112 \rangle$ and $\langle 001 \rangle$ type of jog vectors on the screw dislocation.

3.1. The core structure of a $\frac{1}{2}\langle 011 \rangle$ jog on a screw dislocation in FCC Cu and Ni

Fig. 1a depicts the fully relaxed core structure of a dislocation lying along the x direction in FCC Cu. The figure shows that the screw dislocation is fully dissociated into Shockley partials on the (111) glide plane, save for the jog vector that is spread out and dissociated on the $(11-1)$ cross-slip plane. This is a local minimum

energy configuration for the $\frac{1}{2}[011]$ jog. This configuration is termed the ‘extended’ configuration for the jog. Upon application of compressive stresses along the $[11-1]$ direction, the extended jog configuration collapses to the ‘sharp’ configuration shown in Fig. 1b, where the jog vector is compact and not extended. This configuration is more like a classical continuum description of the jog core structure. The sharp jog configuration remains stable even after relaxation of the applied compressive stresses, and has a lower energy compared to the extended configuration of about 0.4 eV. Therefore, the sharp configuration is the global minimum energy structure for the $\frac{1}{2}\langle 011 \rangle$ type jog. The extended configuration has a lower dislocation line length as compared to the sharp configuration; however, it also has two fully developed constrictions as compared to the sharp configuration, for which there is essentially only a single fully developed constriction.

The nudged elastic band method [9] was also used to determine the activation energy required to transform the jog from the sharp to the extended state. This activation energy was also determined to be ~ 0.4 eV, where the extended configuration is at a very shallow local minimum. Therefore, 0.4 eV represents the activation energy for cross-slip at the $\frac{1}{2}\langle 011 \rangle$ cross-slip jog on a screw dislocation in FCC Cu. This is a factor of 4–5 lower than the activation energy for cross-slip of a screw dislocation in isolation without any jogs [10]. The decrease in cross-slip activation energy is mainly a result from the fact that there is a pre-existing constriction on the glide plane at the jog. Fig. 2a and b show the extended and sharp configurations of an $a/2\langle 011 \rangle$ jog on a screw dislocation for FCC Ni. The configurations are very similar to what was obtained for Cu. Similar nudged elastic band method calculations as in Cu show that the activation energy for cross-slip at a jog in FCC Ni is also close to 0.4 eV, a factor of 4–5 lower than the cross-slip activation

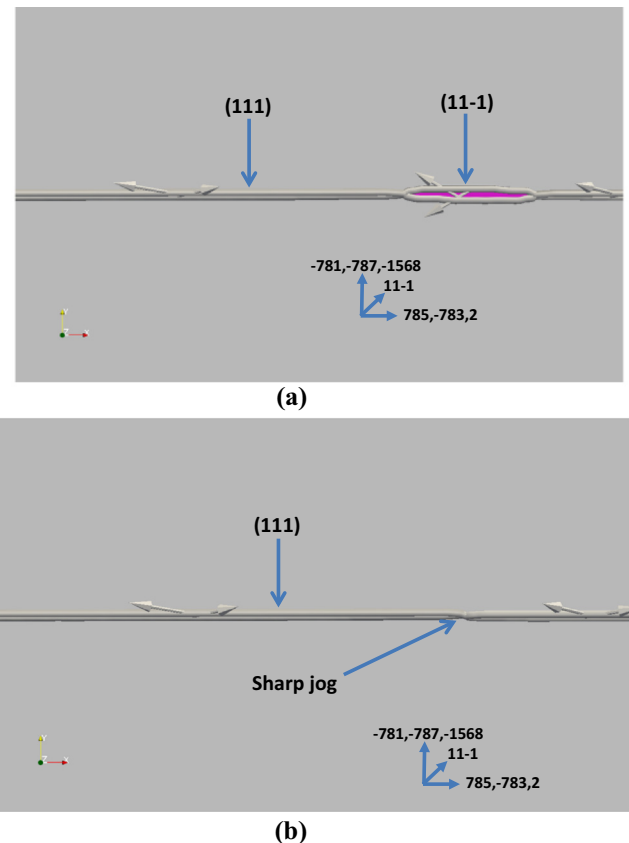


Fig. 1. (a) Extended and (b) sharp configurations of an $\frac{1}{2}\langle 011 \rangle$ cross-slip jog on a $\frac{1}{2}[1-10]$ screw dislocation in FCC Cu, obtained using the Mishin Cu potential [17].

energy of a screw dislocation in the absence of any jogs. Collectively, these findings suggest that cross-slip should preferentially nucleate at pre-existing jogs on screw dislocations in FCC metals.

3.2. Annihilation of jogged-screw dipoles versus temperature and applied stress

Fig. 3a–c show a time sequence of molecular dynamics simulation results for the cross-slip annihilation process of two oppositely signed screw dislocations, one of which contains a $\frac{1}{2}[011]$ sharp atomic jog on the $(11-1)$ cross-slip plane. The screw dislocations are initially separated by 14 nm on the $(11-1)$ cross-slip plane. The initial conditions to the MD simulations was a molecular statics relaxed cell under the same applied stress. They are shown in 2D projections in Fig. 3d where atoms with a centrosymmetry parameter greater than 4 are plotted for the initial molecular statics relaxed cell. The temperature for the simulations was 5 K and, an Escaig stress of 450 MPa was applied on the (111) glide plane. At time $t = 10$ ps, cross-slip has initiated at the atomic jog and part of the screw dislocation near the jog has spread out on the $(11-1)$ cross-slip plane. With further dynamics, the cross-slipped portion of the screw dislocation is attracted toward the oppositely-signed screw dislocation along with further spreading on the cross-slip plane. At time $t = 30$ ps, screw dipole annihilation by cross-slip process is initiated (see Fig. 3a–c). These results suggest that cross-slip preferentially occurs at jogs on screw dislocations in FCC materials.

Fig. 4 summarizes the molecular dynamics simulations results that determine the critical Escaig stresses on the glide plane required for the annihilation of jogged screw dislocations sepa-

rated by either 14 or 44 nm in Cu. The critical Escaig stress sharply decreases with increasing temperature, and at room temperature only a minimum amount of Escaig stress is required for cross-slip initiation and dipole annihilation for both dipole separation distances. Note that these stresses have not been corrected for the much shorter time available for MD simulations as compared to real experiments. Consequently, this suggests that jog-assisted cross-slip is essentially athermal at room temperature in Cu and Ni. Also, the interaction stresses between the two oppositely signed screw dislocations have minimal effect on the critical Escaig stress for dipole annihilation by cross-slip at these separation distances. The critical Escaig stress on the glide plane required for cross-slip initiation at jogs, at 5 K, is approximately 350-to-400 MPa (see Fig. 4). Similar calculations were performed at 5 K for two other stress components: (a) Escaig stress on cross-slip plane and (b) glide stress on cross-slip plane. The critical stress required for jogged screw dipole annihilation or cross-slip initiation at jogs for these two stress components is approximately 575 and 900 MPa (see Fig. 4). Assuming a linear dependence of cross-slip activation energy at jogs as a function of these three stress components,

$$H = H_0(0.4 \text{ eV}) - V_i \tau_i$$

where τ_i is one of the three stress components and V_i is the activation volume of the cross-slip activation energy with respect to one of the three stress components, the activation volume for cross-slip at a jog can be deduced from the critical stresses at 5 K as ranging between 6 and $20b^3$, where b is the magnitude of the Burgers vector.

If the oppositely-signed jogged screw dislocations, in addition to being separated by 14 or 44 nm along the glide plane normal, are also separated along the $[11-2]$ direction on the glide plane by a certain amount, the interaction forces between the two screws make them glide toward each other along the $[11-2]$ direction. However, the $\frac{1}{2}[011]$ jog on the cross-slip plane is immobile on the glide plane. This results in the dragging of an edge dipole from the $\frac{1}{2}[011]$ jog as the screw dislocations glide toward each other (see Fig. 5). Such dipole dragging has been observed experimentally during deformation of single crystalline FCC materials [19]. Once this occurs, cross-slip nucleation at the jog is prohibitively difficult. This observation suggests that cross-slip initiation at atomic jogs is favorable only under specialized conditions in FCC materials.

4. Discussion

This work shows that the activation energy for nucleation of cross-slip at jogs on screw-character dislocations of an FCC metal under favorable conditions, is a factor of 4 to 5 times lower than the initiation of cross-slip on an isolated straight screw dislocation. Further, this work along with previous calculations on mildly attractive and repulsive screw dislocation intersections provides a methodology to obtain the variation in nucleation barrier for cross-slip within a given system. These calculations, along with results from our prior work [8–12], have been implemented in large-scale 3D dislocation dynamics simulations and used to obtain realistic cross-slip statistics at different length scales [20]. The results have proven to permit improved simulations of metallic behavior such as strain hardening and fatigue [20] that have not been possible without ad-hoc assumptions about cross-slip.

The results clearly show that cross-slip nucleation at jogs on screw dislocations is significantly easier than cross-slip nucleation in the absence of jogs, having an activation energy, a factor of 4–5 lower in Cu and Ni. The current result rationalizes the experimentally-observed profuse nature of cross slip in FCC crystals in a more satisfactory manner than the previous models of

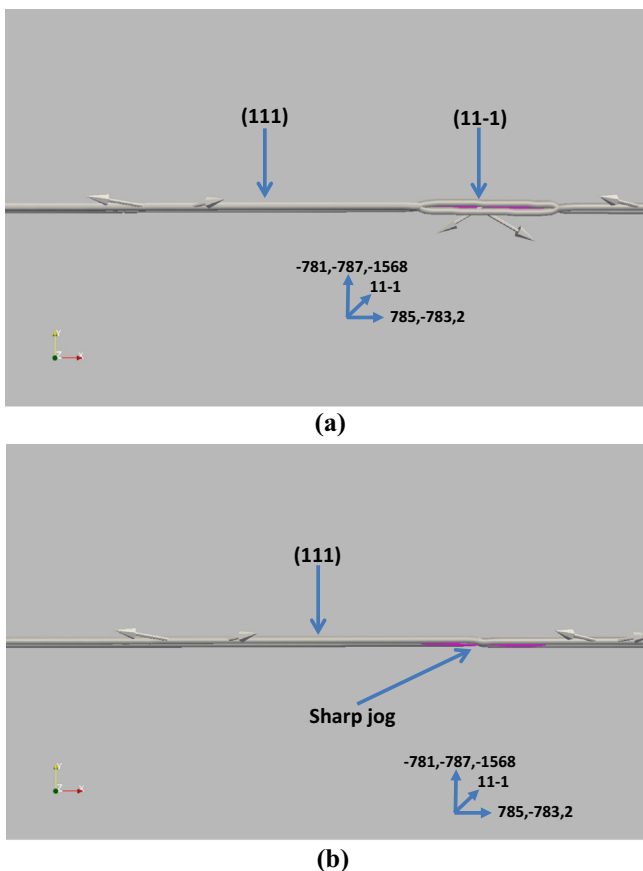


Fig. 2. (a) Extended and (b) sharp configurations of an $\frac{1}{2}[011]$ cross-slip jog on a $\frac{1}{2}(1-1)$ screw dislocation in FCC Ni, obtained using the Mishin Ni potential [16].

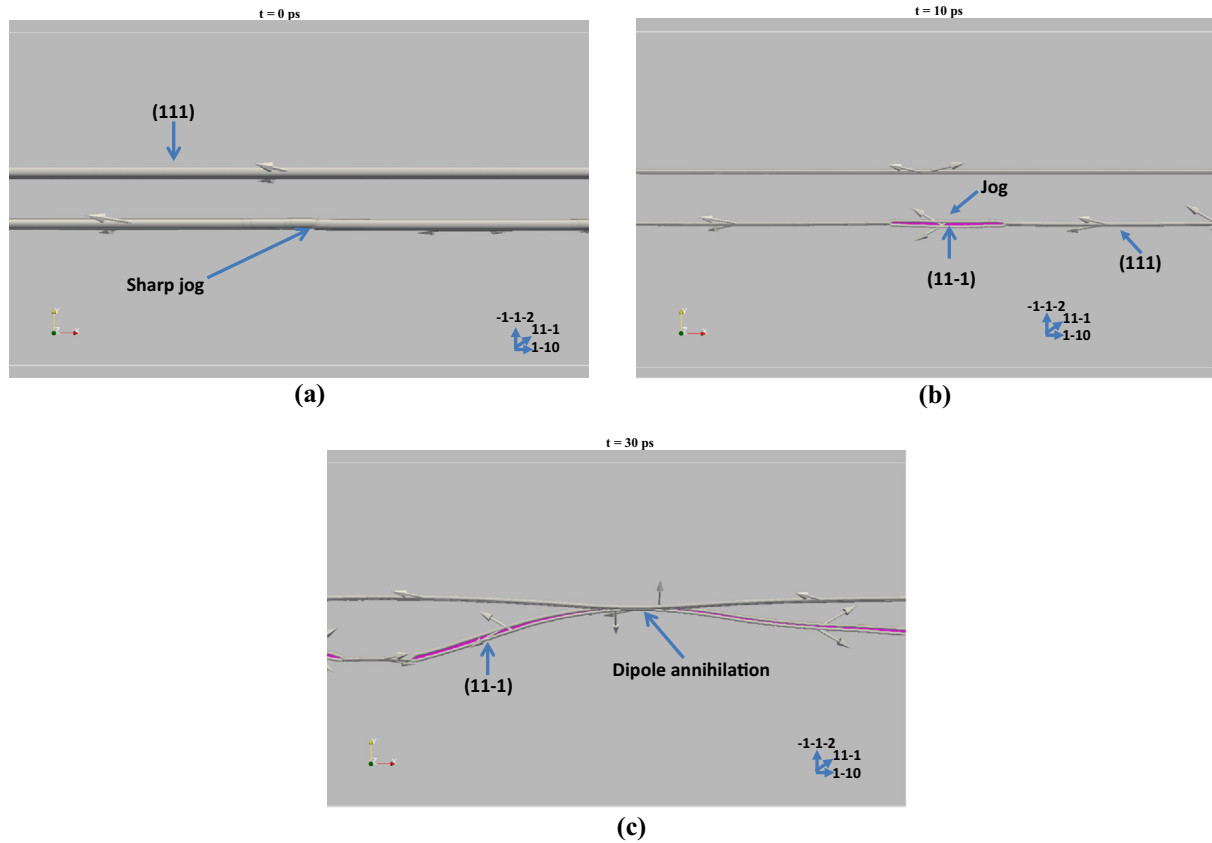


Fig. 3a–c. A time sequence of the annihilation process of two oppositely signed $a/2\langle 1-10 \rangle$ screw dislocations, separated by 14 nm on the $(11-1)$ cross-slip plane in FCC Cu, (a) 0 ps, (b) 10 ps and (c) 30 ps. One of the screw dislocations contains a $\frac{1}{2}\langle 011 \rangle$ atomic cross-slip jog

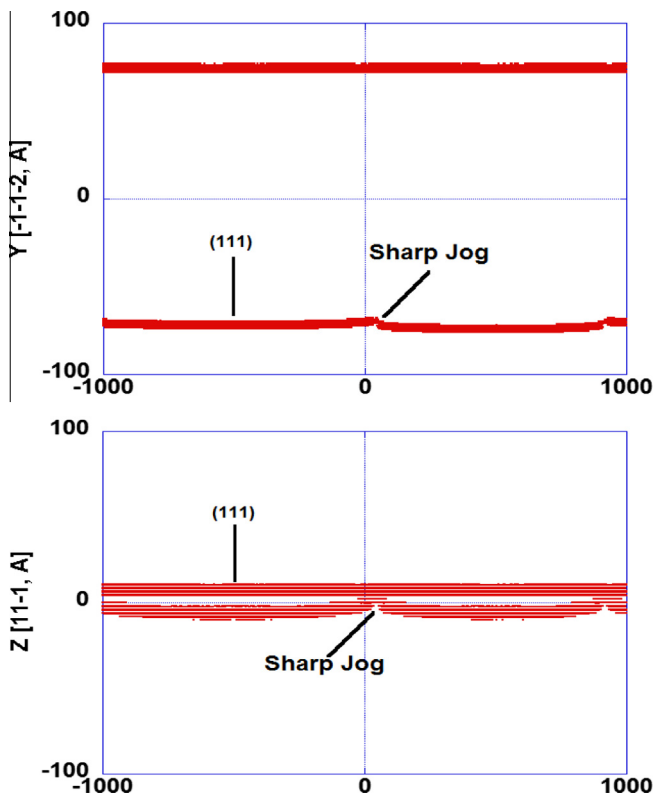


Fig. 3d. $(11-1)$ and $(-1-1-2)$ projections of the initial conditions to the dipole annihilation MD simulations shown in a. Atoms with a centrosymmetry parameter less than 4 are shown in the figure.

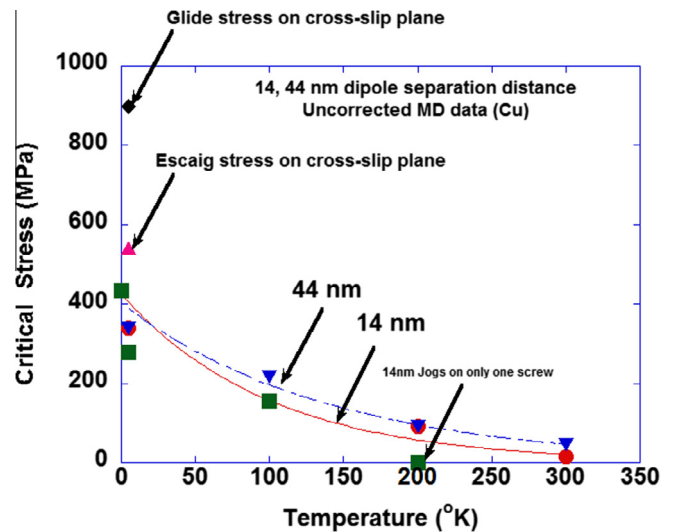


Fig. 4. Critical Escaig stresses on the glide plane required for the annihilation of two oppositely-signed jogged $\frac{1}{2}\langle 1-10 \rangle$ screw dislocations separated by 14 and 44 nm on the $[11-1]$ cross-slip plane, as a function of temperature. Also, shown are the critical Escaig stress on the cross-slip plane and critical glide stress on the cross-slip plane for the jogged screw dislocation annihilation process at 5 K.

thermally-activated cross slip. Those models all require too high of stress to provide a self-consistent explanation. However, glide stresses acting on the screw dislocation tend to drag out edge dipoles at the jog and make cross-slip prohibitively difficult under such conditions.

In conclusion, we reiterate the merits of higher-level simulations that incorporate these new mechanisms. These mechanisms

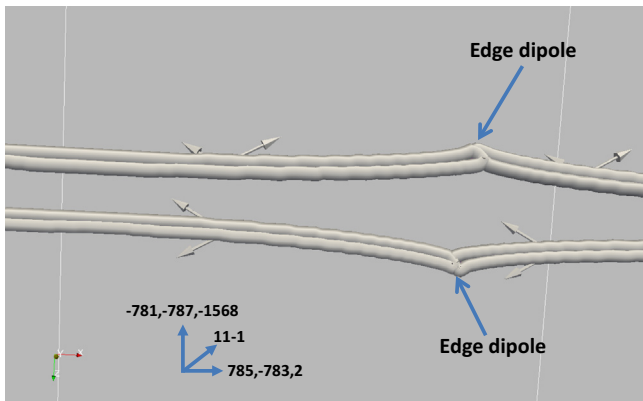


Fig. 5. Edge dipole dragging at $\frac{1}{2}\langle 011 \rangle$ jogs on $\frac{1}{2}\langle 1-10 \rangle$ screw dislocations in FCC Cu in the presence of interaction stresses on the $\langle 111 \rangle$ glide plane.

of cross-slip slip for screw dislocations, along with previously-published intersection mechanism of cross-slip nucleation, have been implemented in 3D dislocation dynamics simulations as an alternative to Escaig's model for FCC materials. The augmented dislocation dynamics simulations accounting for these new mechanisms of cross-slip have shown realistic cell structure formation in $5\ \mu\text{m}$ diameter simulation cells deformed to 0.5% strain under multislip conditions [20]. Such cell structure formation and dislocation microstructure evolution with strain has been shown to be largely absent in the absence of cross-slip [20]. Also, dislocation dynamics simulations accounting for the newly determined mechanisms of cross-slip show realistic strain-hardening rates as a function of orientation of deformation $[001]$, $[111]$ and $[110]$ crystal directions in larger $20 \times 20 \times 50\ \mu\text{m}$ simulation cells [21]. The strain-hardening rates within the regime of the elastic to plastic transition, extending to $\sim 1\%$ shear strain and, the relative changes in magnitude of work-hardening rates as a function of orientation, are in reasonable accord with experimental data acquired at room temperature [21]. Such simulations should be performed as a function of deformation temperature and compared with corresponding experimental stress-strain and dislocation microstructure data, to test whether the activation energies and cross-slip mechanisms deduced from present and previous [21] atomistic simulations can be brought into quantitative agreement with experimental measurements.

5. Summary

Large-scale atomistic simulations were used to examine the effect of jogs on the cross-slip of screw dislocations and screw-dipole annihilation in Cu and Ni. From these simulations, the following conclusions are drawn.

- (1) The stress-free activation energy for cross-slip of screw dislocations at jogs is approximately 0.4 eV in FCC Cu and Ni; a factor of 4–5 lower than the activation energy for cross-slip of screw dislocations in the absence of a jog.
- (2) The critical Escaig stress on the glide plane for jogged screw dipole annihilation drops from the 0 K value (~ 400 MPa) to ~ 0 at room temperature, and dipole annihilation is nearly athermal at room temperature.
- (3) At 5 K, Escaig stresses on the cross-slip plane are a factor of 1.5 less effective than Escaig stresses on the glide plane and, glide stresses on the cross-slip plane are a factor of 3 less effective for dipole annihilation by cross-slip.
- (4) The activation volume for cross-slip of screw dislocations at jogs with respect to these three stress components range from 20 to $6b^3$.

These results – along with previously published simulation results on intersection cross-slip nucleation in FCC crystals [8–12] – have been found useful in physics-based modeling of cross-slip in higher length scale 3D dislocation dynamics simulations that have investigated dislocation pattern formation and fatigue structures in FCC crystals [20,21].

Acknowledgements

The authors acknowledge use of the 3D molecular dynamics code, LAMMPS, that was developed at Sandia National Laboratory by Dr. Steve Plimpton and co-workers. The authors acknowledge useful discussions with Dr. L.P. Kubin of ONERA and Prof. L.M. Brown of Cambridge University during the course of this work. This work was supported by AFOSR (Dr. David Stargel), and by a grant of computer time from the DOD High Performance Computing Modernization Program, at the Aeronautical Systems Center/Major Shared Resource Center. The work was performed at the U.S. Air Force Research Laboratory, Materials and Manufacturing Directorate, Wright-Patterson AFB.

References

- [1] W. Puschl, Models for dislocation cross-slip in close packed crystal structures: a critical review, *Prog. Mater. Sci.* 47 (2002) 415.
- [2] P.J. Jackson, Dislocation modelling of shear in fcc crystals, *Prog. Mater. Sci.* 29 (1985) 139.
- [3] J. Bonneville, B. Escaig, Cross-slipping process and the stress-orientation dependence in pure copper, *Acta Metall.* 27 (1979) 1477.
- [4] J. Bonneville, B. Escaig, J.L. Martin, A study of cross-slip activation parameters in pure copper, *Acta Metall.* 36 (1988) 1989.
- [5] B. Escaig, in: A.R. Rosenfield, G.T. Hahn, A.L. Bement Jr., R.I. Jaffee (Eds.), *Proceedings of the Battelle Colloquium on Dislocation Dynamics*, McGraw-Hill, New York, 1968, p. 655.
- [6] D. Caillard, J.L. Martin, *Thermally Activated Mechanisms in Crystal Plasticity*, Pergamon-Elsevier, Amsterdam, 2003.
- [7] G. Saada, Cross-slip and work hardening of fcc crystals, *Mater. Sci. Eng., A* 137 (1991) 177.
- [8] S. Rao, D.M. Dimiduk, J. El-Awady, T.A. Parthasarathy, M.D. Uchic, C. Woodward, Atomistic simulations of cross-slip nucleation at screw dislocation intersections in face-centered cubic nickel, *Phil. Mag.* 89 (34) (2009) 3351.
- [9] S. Rao, D.M. Dimiduk, J. El-Awady, T.A. Parthasarathy, M.D. Uchic, C. Woodward, Activated states for cross-slip at screw dislocation intersections in face-centered cubic nickel and copper via atomistic simulation, *Acta Mater.* 58 (2010) 5547.
- [10] S. Rao, D.M. Dimiduk, T.A. Parthasarathy, J. El-Awady, M.D. Uchic, C. Woodward, Calculation of intersection cross-slip activation energies in fcc metals using nudged elastic band method, *Acta Mater.* 59 (2011) 7135.
- [11] S.I. Rao, D.M. Dimiduk, T.A. Parthasarathy, M.D. Uchic, C. Woodward, Atomistic simulations of intersection cross-slip nucleation in $L1_2$ Ni₃Al, *Scr. Mater.* 66 (2012) 410.
- [12] S.I. Rao, D.M. Dimiduk, J.A. El-Awady, T.A. Parthasarathy, M.D. Uchic, C. Woodward, Spontaneous athermal cross-slip nucleation at screw dislocation intersections in fcc metals and $L1_2$ intermetallics investigated via atomistic simulations, *Phil. Mag.* 93 (2013) 3012.
- [13] T. Vegge, K.W. Jacobsen, Atomistic simulations of dislocation processes in copper, *J. Phys. Condens. Matter* 14 (2002) 2929.
- [14] T. Vegge, T. Rasmussen, T. Leffers, O.B. Pedersen, K.W. Jacobsen, Atomistic simulations of cross-slip of jogged screw dislocations in copper, *Phil. Mag. Lett.* 81 (2001) 137.
- [15] S.J. Plimpton, Fast parallel algorithms for short-range molecular dynamics, *J. Comp. Phys.* 117 (1995) 1.
- [16] Y. Mishin, Atomistic modeling of the γ and γ' -phases of the Ni–Al system, *Acta Mater.* 52 (2004) 1451.
- [17] Y. Mishin, M.J. Mehl, D.A. Papaconstantopoulos, A.F. Voter, J.D. Kress, Structural stability and lattice defects in copper: ab-initio, tight-binding and embedded-atom calculations, *Phys. Rev. B* 63 (2001) 224106.
- [18] A. Stukowski, K. Albe, Extracting dislocations and non-dislocation crystal defects from atomistic simulation data, *Model. Simul. Mater. Sci. Eng.* 18 (2010) 085001.
- [19] J.A. Antonopolos, A.T. Winter, Weak-beam study of dislocation structures in fatigued copper, *Phil. Mag.* 33 (1976) 87.
- [20] A.M. Hussein, S.I. Rao, M.D. Uchic, D.M. Dimiduk, J.A. El-Awady, Microstructurally based cross-slip mechanisms and their effects on dislocation microstructure evolution in fcc crystals, *Acta Mater.* 85 (2015) 180.
- [21] S. Rao, D.M. Dimiduk, Jaafar El-Awady, A. Hussein, T.A. Parthasarathy, M.D. Uchic, C. Woodward, in preparation (2015).